High speed silicon electro-optical modulators enhanced via slow light propagation

A. Brimont,[1,4,*] D. J. Thomson,[2,4] P. Sanchis,[1,4] J. Herrera,[1] F.Y. Gardes,[2] J. M. Fedeli,[3] G. T. Reed,[2] J. Martí,[1]

[1] Nanophotonics Technology Center, Universitat Politécnica de Valencia, Camino de Vera, s/n 46022 Valencia
[2] *Advanced Technology Institute, University of Surrey, Guildford, Surrey, GU2 7XH, UK*
[3] *CEA, LETI, Minatec Campus, 17 Rue des Martyrs, 38054, GRENOBLE Cedex, France*
[4]*These authors contributed equally to this work*
[*]*abrimont@ntc.upv.es*

Abstract: While current optical communication networks efficiently carry and process huge amounts of digital information over large and medium distances, silicon photonics technology has the capacity to meet the ceaselessly increasing demand for bandwidth via energy efficient, inexpensive and mass producible short range optical interconnects. In this context, handling electrical-to-optical data conversion through compact and high speed electro-optical modulators is of paramount importance. To tackle these challenges, we combine the attractive properties of slow light propagation in a nanostructured periodic waveguide together with a high speed semiconductor *pn* diode, and demonstrate a highly efficient and mass manufacturable 500 μm-long silicon electro-optical device, exhibiting error free modulation up to 20 Gbit/s. These results, supported by modulation rate capabilities reaching 40 Gbit/s, pave a foreseeable way towards dense, low power and ultra fast integrated networks-on-chip for future chip-scale high performance computing systems.

OCIS codes: (250.5300) Photonic integrated circuits; (350.4238) Nanophotonics and photonic crystals; (250.4110) Modulators.

References and links

1. M. Asghari and A. V. Krishnamoorthy, "Silicon photonics: Energy-efficient communication," Nat. Photonics **5**(5), 268–270 (2011).
2. R. S. Jacobsen, K. N. Andersen, P. I. Borel, J. Fage-Pedersen, L. H. Frandsen, O. Hansen, M. Kristensen, A. V. Lavrinenko, G. Moulin, H. Ou, C. Peucheret, B. Zsigri, and A. Bjarklev, "Strained silicon as a new electro-optic material," Nature **441**(7090), 199–202 (2006).
3. J. Liu, M. Beals, A. Pomerene, S. Bernardis, R. Sun, J. Cheng, L. C. Kimerling, and J. Michel, "Waveguide-integrated, ultralow-energy GeSi electro-absorption modulators," Nat. Photonics **2**(7), 433–437 (2008).
4. M. Liu, X. Yin, E. Ulin-Avila, B. Geng, T. Zentgraf, L. Ju, F. Wang, and X. Zhang, "A graphene-based broadband optical modulator," Nature **474**(7349), 64–67 (2011).
5. G. T. Reed, G. Mashanovich, F. Y. Gardes, and D. J. Thomson, "Silicon optical modulators," Nat. Photonics **4**(8), 518–526 (2010).
6. R. A. Soref and B. R. Bennett, "Electrooptical Effects in Silicon," IEEE J. Quantum Electron. **23**(1), 123–129 (1987).
7. A. Liu, R. Jones, L. Liao, D. Samara-Rubio, D. Rubin, O. Cohen, R. Nicolaescu, and M. Paniccia, "A high-speed silicon optical modulator based on a metal-oxide-semiconductor capacitor," Nature **427**(6975), 615–618 (2004).
8. L. Liao, D. Samara-Rubio, M. Morse, A. Liu, D. Hodge, D. Rubin, U. Keil, and T. Franck, "High speed silicon Mach-Zehnder modulator," Opt. Express **13**(8), 3129–3135 (2005).
9. W. M. Green, M. J. Rooks, L. Sekaric, and Y. A. Vlasov, "Ultra-compact, low RF power, 10 Gb/s silicon Mach-Zehnder modulator," Opt. Express **15**(25), 17106–17113 (2007).
10. S. Manipatruni, X. Qianfan, B. Schmidt, J. Shakya, and M. Lipson, "High Speed Carrier Injection 18 Gb/s Silicon Micro-ring Electro-optic Modulator," in *Lasers and Electro-Optics Society, 2007. LEOS 2007. The 20th Annual Meeting of the IEEE*, 2007), 537–538.
11. L. Liao, A. Liu, J. Basak, H. Nguyen, M. Paniccia, D. Rubin, Y. Chetrit, R. Cohen, and N. Izhaky, "40 Gbit/s silicon optical modulator for high speed applications," Electron. Lett. **43**(22), 1196 (2007).
12. F. Y. Gardes, A. Brimont, P. Sanchis, G. Rasigade, D. Marris-Morini, L. O'Faolain, F. Dong, J. M. Fedeli, P. Dumon, L. Vivien, T. F. Krauss, G. T. Reed, and J. Martí, "High-speed modulation of a compact silicon ring resonator based on a reverse-biased pn diode," Opt. Express **17**(24), 21986–21991 (2009).

#149714 - $15.00 USD Received 22 Jun 2011; revised 22 Jul 2011; accepted 25 Jul 2011; published 5 Oct 2011

13. P. Dong, S. Liao, H. Liang, W. Qian, X. Wang, R. Shafiiha, D. Feng, G. Li, X. Zheng, A. V. Krishnamoorthy, and M. Asghari, "High-speed and compact silicon modulator based on a racetrack resonator with a 1 V drive voltage," Opt. Lett. **35**(19), 3246–3248 (2010).
14. D. J. Thomson, F. Y. Gardes, Y. Hu, G. Mashanovich, M. Fournier, P. Grosse, J. M. Fedeli, and G. T. Reed, "High contrast 40Gbit/s optical modulation in silicon," Opt. Express **19**(12), 11507–11516 (2011).
15. H.-W. Chen, J. D. Peters, and J. E. Bowers, "Forty Gb/s hybrid silicon Mach-Zehnder modulator with low chirp," Opt. Express **19**(2), 1455–1460 (2011).
16. L. Alloatti, D. Korn, R. Palmer, D. Hillerkuss, J. Li, A. Barklund, R. Dinu, J. Wieland, M. Fournier, J. Fedeli, H. Yu, W. Bogaerts, P. Dumon, R. Baets, C. Koos, W. Freude, and J. Leuthold, "42.7 Gbit/s electro-optic modulator in silicon technology," Opt. Express **19**(12), 11841–11851 (2011).
17. J. A. Dionne, K. Diest, L. A. Sweatlock, and H. A. Atwater, "PlasMOStor: a metal-oxide-Si field effect plasmonic modulator," Nano Lett. **9**(2), 897–902 (2009).
18. L. V. Hau, S. E. Harris, Z. Dutton, and C. H. Behroozi, "Light speed reduction to 17 metres per second in an ultracold atomic gas," Nature **397**(6720), 594–598 (1999).
19. P.-C. Ku, F. Sedgwick, C. J. Chang-Hasnain, P. Palinginis, T. Li, H. Wang, S.-W. Chang, and S.-L. Chuang, "Slow light in semiconductor quantum wells," Opt. Lett. **29**(19), 2291–2293 (2004).
20. M. González Herráez, K. Y. Song, and L. Thévenaz, "Arbitrary-bandwidth Brillouin slow light in optical fibers," Opt. Express **14**(4), 1395–1400 (2006).
21. M. Notomi, K. Yamada, A. Shinya, J. Takahashi, C. Takahashi, and I. Yokohama, "Extremely large group-velocity dispersion of line-defect waveguides in photonic crystal slabs," Phys. Rev. Lett. **87**(25), 253902 (2001).
22. H. Gersen, T. J. Karle, R. J. P. Engelsen, W. Boa, J. P. Korterik, N. F. Hulst, T. F. Krauss, and L. Kuipers, "Real-Space Observation of Ultraslow Light in Photonic Crystal Waveguides," Phys. Rev. Lett. **94**(7), 073901–073904 (2005).
23. Y. A. Vlasov, M. O'Boyle, H. F. Hamann, and S. J. McNab, "Active control of slow light on a chip with photonic crystal waveguides," Nature **438**(7064), 65–69 (2005).
24. G. von Freymann, S. John, S. Wong, V. Kitaev, and G. A. Ozin, "Measurement of group velocity dispersion for finite size three-dimensional photonic crystals in the near-infrared spectral region," Appl. Phys. Lett. **86**(5), 053108–053103 (2005).
25. H. F. Taylor, "Enhanced Electrooptic Modulation Efficiency Utilizing Slow-Wave Optical Propagation," J. Lightwave Technol. **17**(10), 1875–1883 (1999).
26. M. Soljačić, S. G. Johnson, F. Shanhui, M. Ibanescu, E. Ippen, and J. D. Joannopoulos, "Photonic-crystal slow-light enhancement of nonlinear phase sensitivity," J. Opt. Soc. Am. B **19**(9), 2052–2059 (2002).
27. Y. Jiang, W. Jiang, L. Gu, X. Chen, and R. T. Chen, "80-micron interaction length silicon photonic crystal waveguide modulator," Appl. Phys. Lett. **87**(22), 221105 (2005).
28. L. Gu, W. Jiang, X. chen, L. Wang, and R. T. Chen, "High speed silicon photonic crystal waveguide modulator for low voltage operation," Appl. Phys. Lett. **90**, 071101–071103 (2007).
29. X. Chen, Y.-S. Chen, Y. Zhao, W. Jiang, and R. T. Chen, "Capacitor-embedded 0.54 pJ/bit silicon-slot photonic crystal waveguide modulator," Opt. Lett. **34**(5), 602–604 (2009).
30. L. O'Faolain, D. M. Beggs, T. P. White, T. Kampfrath, K. Kuipers, and T. F. Krauss, "Compact Optical Switches and Modulators Based on Dispersion Engineered Photonic Crystals," IEEE Photon. J. **2**(3), 404–414 (2010).
31. A. Brimont, P. Sanchis, and J. Martí, "Strong electro-optical modulation enhancement in a slow wave corrugated waveguide," Opt. Express **17**(11), 9204–9211 (2009).
32. D. J. Thomson, F. Y. Gardes, G. T. Reed, F. Milesi, and J. M. Fedeli, "High speed silicon optical modulator with self aligned fabrication process," Opt. Express **18**(18), 19064–19069 (2010).
33. E. Kuramochi, M. Notomi, S. Hughes, A. Shinya, T. Watanabe, and L. Ramunno, "Disorder-induced scattering loss of line-defect waveguides in photonic crystal slabs," Phys. Rev. B **72**(16), 161318 (2005).
34. L. O'Faolain, T. P. White, D. O'Brien, X. Yuan, M. D. Settle, and T. F. Krauss, "Dependence of extrinsic loss on group velocity in photonic crystal waveguides," Opt. Express **15**(20), 13129–13138 (2007).
35. S. Hughes, L. Ramunno, J. F. Young, and J. E. Sipe, "Extrinsic optical scattering loss in photonic crystal waveguides: role of fabrication disorder and photon group velocity," Phys. Rev. Lett. **94**(3), 033903 (2005).
36. L. H. Frandsen, A. V. Lavrinenko, J. Fage-Pedersen, and P. I. Borel, "Photonic crystal waveguides with semi-slow light and tailored dispersion properties," Opt. Express **14**(20), 9444–9450 (2006).
37. S. Kubo, D. Mori, and T. Baba, "Low-group-velocity and low-dispersion slow light in photonic crystal waveguides," Opt. Lett. **32**(20), 2981–2983 (2007).
38. M. D. Settle, R. J. P. Engelen, M. Salib, A. Michaeli, L. Kuipers, and T. F. Krauss, "Flatband slow light in photonic crystals featuring spatial pulse compression and terahertz bandwidth," Opt. Express **15**(1), 219–226 (2007).
39. A. Brimont, J. V. Galán, J. M. Escalante, J. Martí, and P. Sanchis, "Group-index engineering in silicon corrugated waveguides," Opt. Lett. **35**(16), 2708–2710 (2010).

1. Introduction

Today's long and medium range communication networks rely mainly on optical fiber links where encoding electrical signals into near-infrared modulated light is an essential function traditionally realized by discrete electro-optical modulators. The growing trend of carrying information over much shorter distances coupled to the foreseen microelectronics copper interconnect bottleneck has pushed researchers to move towards silicon as an alternative

#149714 - $15.00 USD Received 22 Jun 2011; revised 22 Jul 2011; accepted 25 Jul 2011; published 5 Oct 2011

photonic material [1]. This is due to its capacity to meet the ever increasing demand for high-bandwidth technologies, via ultra fast, energy efficient, small footprint optical networks-on-chip and above all, cost-effectiveness compared to its III-V compound counterparts. However, silicon's natural centro-symmetric crystalline structures rules out any linear electro-optic Pockels effect, conventionally used as a modulation mechanism in commercial lithium niobate modulators, for instance. Although breaking the crystal symmetry by depositing a straining layer on top of a silicon waveguide was demonstrated as a means to induce the linear electro-optic effect [2], no further evidences on devices based on this process have been reported. Alternatively, the combination of complementary-metal-oxide-semiconductor (CMOS) compatible materials such as germanium [3] and very recently graphene [4] with silicon enabled high bandwidth electro-absorption modulators.

Up to date, the free-carrier dispersion effect is the most effective mechanism to achieve high-speed electro-optical modulation in silicon [5]. Basically, it is related to the variations in concentration of free carriers in a semiconductor altering both the real and imaginary parts of the refractive index [6]. Since the first silicon modulator exceeding a 1 GHz bandwidth was demonstrated based on this effect [7], numerous devices have been reported by either accumulation [8], injection [9, 10] or depletion [11–13] of free carriers. Recently, a transmission rate of 40 Gbit/s was reported using both compact (1mm long) and large footprint (3.5mm long) Mach-Zehnder interferometer (MZI) modulators based on carrier depletion operation [14]. However, for the compact version of the device, the state-of-the-art bit rate performance was achieved with a lower ER of 3.5dB, making error free modulation essentially unviable. It should be pointed out that the Bit-Error-rate (BER) measurement stands for the critical performance evaluation test to properly assess the maximum data rate of the modulator in real digital transmission systems. To bypass this issue, silicon-III-V compounds hybrid [15] and silicon-organic hybrid (SOH) [16] modulators were shown to exhibit error free modulation at or around 40 Gbit/s. On the other hand, the need for further reductions in device footprint as well as power consumption has motivated research efforts towards optical resonator-based modulators although maximum data bit rates around 12.5 Gbit/s [13] and up to 18 Gbit/s [10] have been achieved until now. The combination of plasmonics with silicon has also been shown as a promising candidate to push even further the limits of electro-optical modulation [17].

Nevertheless, in all above mentioned approaches the overall modulation performance is ultimately dependent upon the stringent requirement of increasing light-matter interactions. In this context, slow light, i.e. as the group velocity of light propagating through a specific medium is notably slowed down, provides an effective way to achieve compactness and ultra-fast operation when combined with high speed free carrier dynamics. Let us remind that the group velocity of light is defined by $v_g = c/n_g$, where n_g is the group index, which provides an estimate on how much the group velocity of a wavepacket propagating through a dispersive material is reduced compared to the speed of light in a vacuum c. The slow light phenomenon was first and foremost shown in atomic media by electromagnetically induced transparency [18], in semiconductors exhibiting population oscillations [19], as well as by excitation of acoustic waves in fibers [20]. Likewise, silicon-on-insulator (SOI) technology provides an effective platform to produce slow light "on-chip" in 1, 2 or even 3 dimensional periodic structures, where the dielectric periodicity is usually achieved via ordered nanostructuring [21–24]. Since the use of slow light as a means to enhance the sensitivity of photonic integrated active devices was first proposed over a decade ago [25, 26], several works reported preliminary proofs of the benefit of using slow light in association with active functionalities [27–31]. However, up to date, no work has presented thorough experimental evidence of the ground breaking impact of slow light on electro-optic modulators under high speed operation. Here, we show that the modulation efficiency improvement together with a high speed carrier depletion mechanism results in realizing a state-of-the-art ultra compact and fast CMOS slow wave modulator achieving error free transmission (BER $<10^{-9}$) along with moderate insertion losses. Further characterization shows that the modulator performance is not intrinsically limited to this data transmission rate and may clearly be

#149714 - $15.00 USD Received 22 Jun 2011; revised 22 Jul 2011; accepted 25 Jul 2011; published 5 Oct 2011

improved by matching the speed of the electrical modulating signal to that of the optical propagating slow wave.

2. Device overview

Slow light propagation is achieved through the use of a one-dimensional (1D) periodic structure consisting of a laterally corrugated waveguide, with narrow and wide sections of width W=300nm and W_e=650nm, which are repeated over a period a=310nm, as shown in Fig. 1(a), (b). The slow wave waveguide height is H=220nm, which after partial dry etching process leaves a 100nm thick slab (designated h in Fig. 1(c), (d)). Optical phase modulation is achieved by depleting the majority carriers from a reverse biased self aligned *pn* junction [32] connected to highly doped *p*+ and *n*+ regions. These are situated respectively at a distance of S_n=550nm and S_p=500nm from the edge of the narrow waveguide section and covered with compound AlCu electrodes in order to ensure good ohmic contacts. Net doping concentrations in the *p*- and *n-type* regions reached respectively 3.10^{17} at/cm^{-3} and $1.5.10^{18}$ at/cm^{-3}. Highly *p*+ and *n*+ doped regions were implanted both at a concentration of 1.10^{20} at/cm^{-3}.

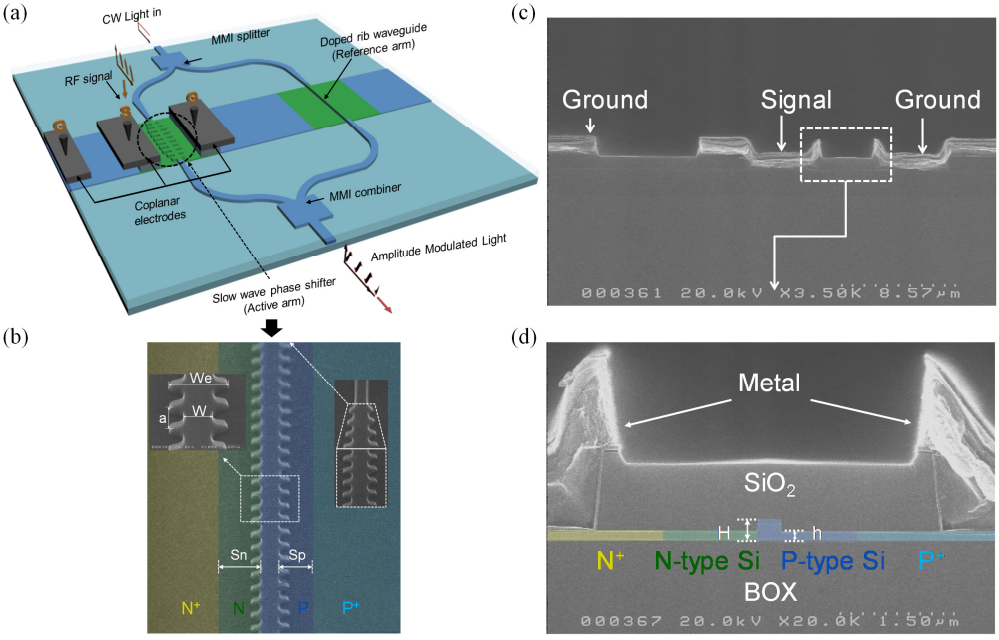

Fig. 1. Overview of the slow wave modulator. (a) Schematic of the modulator based on an asymmetric Mach-Zehnder interferometer (MZI). Multi-mode interference (MMI) structures are used to split and combine the light respectively at the input and output of the MZI. (b) Transverse scanning electron microscope (SEM) picture of the slow wave modulator with an overview of the ground-signal-ground coplanar (GSG) metal electrodes. (c), (d) Top and transverse SEM pictures of the corrugated waveguide. Left inset shows a zoomed view of the taper used to reduce the coupling losses at the rib to slow wave waveguide transitions. Right inset depicts a zoomed view of the corrugated waveguide. Doping regions are delimited by the colored areas.

Slow light interacting with the variable concentration of free carriers is the effect intended to be used as a means to increase light-matter interactions, thus enhancing the modulation efficiency. Figure 1(c), (d) show also the schematic of the designed slow wave modulator as well as scanning electronic microscope (SEM) images of the fabricated structure. Optical phase modulation in the slow wave waveguide is converted into amplitude modulation via the use of an asymmetric MZI. The slow wave phase shifter is placed in the shorter arm of the MZI while a conventional rib waveguide with the same length and doping conditions is placed in the longer arm as a reference. This configuration allowed us to extract both phase

#149714 - $15.00 USD Received 22 Jun 2011; revised 22 Jul 2011; accepted 25 Jul 2011; published 5 Oct 2011

shift variations and insertion losses as a function of the group index from the measured transmission spectra

3. Static performance

Figure 2(a) shows the MZI slow wave modulator normalized transmission spectra under varying reverse bias voltage. The device contains a 1mm long slow wave phase shifter. The free spectral range (FSR) variations across wavelength can be used to extract the group index of the slow wave waveguide [23]. Hence, the group index is calculated as follows:

$$n_{sw}(\lambda) = \left(\frac{n_{ref} \cdot L_{ref} + n \cdot \Delta L}{L_{sw}} \right) \pm \frac{\lambda^2}{FSR \cdot L_{sw}} \quad (1)$$

where λ is the central wavelength of the FSR, n_{sw}, n_{ref}, and n are the respective group indices of the slow wave, 300nm wide reference rib and 400nm wide rib waveguides, L_{sw} and L_{ref} are the lengths of the slow wave and reference rib waveguides and ΔL stands for the length difference between the MZI arms considering only the 400nm wide rib waveguide. The width of the reference rib waveguide was reduced to match that of the narrow section of the slow wave corrugated waveguide. The parameter values are L_{sw}= L_{ref}=1mm, ΔL=0.9mm, n_{ref}≈3.5 and n≈3.7. The selection of the sign in the right-hand side of Eq. (1) depends upon the considered wavelength range and is related to the fact that the FSR exhibits different behaviors as we move from the fast light region towards the photonic band gap (PBG).

In the fast light regime (far enough from the PBG) the separation between the interference fringes remains approximately constant, which is consistent with a nearly unvarying group index value and the negative sign must be used in Eq. (1). However, as we enter the slow light regime, i.e. as we move closer to PBG, the FSR increases up to a maximum value, which means that the phase difference between the MZI arms is minimized. From this point forward, the positive sign must be used in Eq. (1) because higher group indices imply that the effective optical path length of the shorter arm become larger than that of the longer arm thus causing the FSR to decrease.

As can be observed in Fig. 2(b), the maximum calculated group index value lies around 22 at the edge of PBG, which is better seen in Fig. 2(c). Furthermore, Fig. 2(d) depicts the resultant phase shift variations relative to π radians versus applied reverse bias voltages and for varying group index. As a reference and to demonstrate the enhancement produced by the slow wave effect, a conventional 400nm wide silicon rib phase shifter exhibiting a group index of ~3.7 and embedded in the same *pn* junction with identical doping concentrations has been included on the same sample and characterized. As observed in Fig. 2(d), the corresponding achieved phase shift is approximately the same as that of the slow wave phase shifter biased in the fast light regime, but strongly increases as the group index does within the slow light region. This is because the modulation efficiency $V_\pi L_\pi$, calculated as the average value between 0 and 10V (with 2 V increments), is significantly enhanced. Indeed, although for the conventional phase shifter, the calculated $V_\pi L_\pi$ is ~2.2V·cm, it significantly improves for the slow wave phase shifter, even for moderate group indices. For instance, a $V_\pi L_\pi$~1.27V·cm is obtained for a group index of 11 and as low as ~0.45V·cm when the group index increases up to ~22.

#149714 - $15.00 USD Received 22 Jun 2011; revised 22 Jul 2011; accepted 25 Jul 2011; published 5 Oct 2011

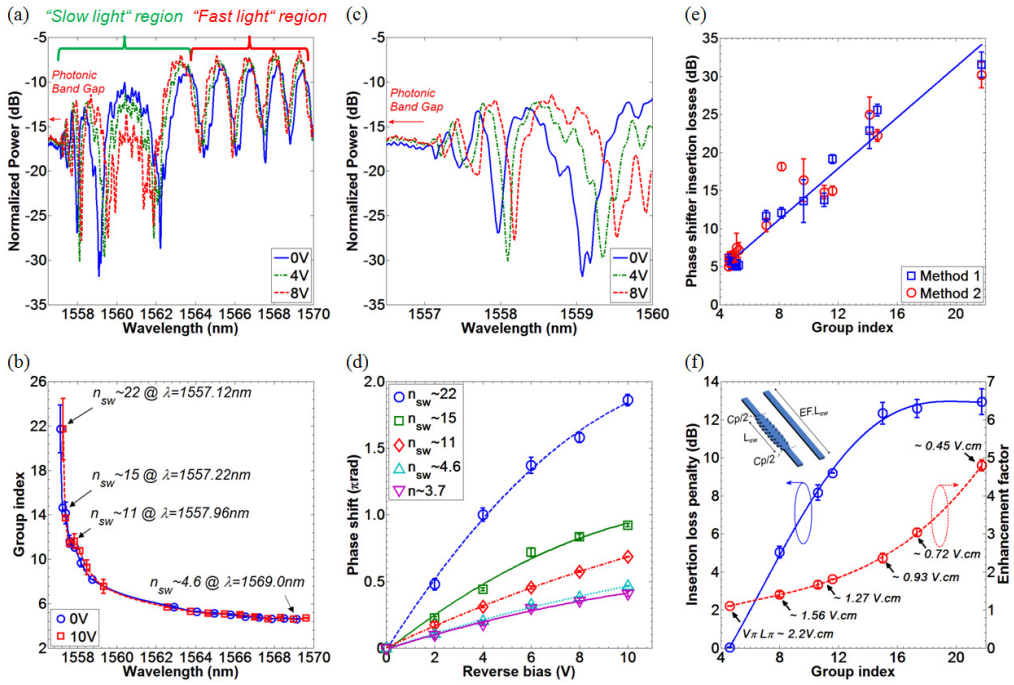

Fig. 2. Static operation of the 1 mm-long slow wave modulator. (a) Normalized transmission spectrum of the slow wave modulator for three different reverse biased voltages. The slow and fast light regions are respectively delimited in green and red. (b) Group index variations versus wavelength at 0V and 10V bias voltages. (c) Expanded view of the slow light region. (d) Phase shift dependence versus applied bias for varying group index. (e) Insertion losses versus group index of the 1mm long slow wave phase shifter. (f) Insertion loss penalty relative to the conventional modulator for a modulation length L_{sw}=1mm and enhancement factor versus group index. C_p accounts for the coupling losses between the slow wave and conventional rib waveguides. The average modulation efficiencies (between 0 and 10 V with 2 V increments) versus group index of the slow wave modulator are also shown for varying group index. V_π and L_π are respectively the bias voltage and modulation length required to achieve a π radian phase shift.

The enhanced modulation efficiency offers two alternatives over the conventional rib modulator. Namely, either a device requiring lower drive voltage while conserving the modulation length or a more compact device requiring the same drive voltage. The second option is a priori preferred for several reasons besides the compactness. Indeed, a shorter modulation length is expected to increase the modulation bandwidth and reduce the insertion losses. The latter is in fact the main limitation of slow wave based devices as increasing the group index will lead to higher losses. Briefly, although their causes and mechanisms have been subject of discussions [23, 33–35], one may point out coupling and slow wave propagation as the main source of losses. Coupling losses originates from the modal mismatch between the fast and slow modes at the rib to slow wave waveguide transitions while propagation losses are a consequence of the stronger interaction of the optical mode with, on one hand fabrication imperfections (essentially sidewall roughness and residual crystalline defects after the implantation process) and, on the other hand free carriers generating higher absorption. Backscattering losses produced by disorder is thought to play a minor role owing to the moderately high group index involved here.

4. Insertion losses

The insertion losses can be estimated from the extinction ratio (ER) variations of the interference fringes using a specific method, here called method 1, which will be reported elsewhere. As an alternative approach, here called method 2, they have also been directly

#149714 - $15.00 USD Received 22 Jun 2011; revised 22 Jul 2011; accepted 25 Jul 2011; published 5 Oct 2011

estimated from the measured transmission spectrum of a single slow wave phase shifter. The two methods show good agreement as depicted in Fig. 2(e). The insertion loss, whose dependence upon group index has been approximated by a linear fitting, increases from ~5 dB in the fast light region (n_{sw}≈4.6), to around 16 dB at n_{sw}≈11 and 34 dB at n_{sw}≈22. However, although there is a significant increase in loss inherent in the use of higher group indices, the total insertion loss penalty in our slow wave modulator with respect to a conventional device may be balanced owing to the fact that smaller modulation lengths are required to achieve a given phase shift. To illustrate this, an enhancement factor has been defined as

$$EF \approx \frac{\Delta\phi_{sw}}{\Delta\phi} \tag{2}$$

where $\Delta\phi_{sw}$ and $\Delta\phi$ are the respective average phase shifts achieved in the slow wave and conventional phase shifters. The enhancement factor, directly related to the modulation efficiency $V_\pi L_\pi$, is shown in Fig. 2 (f) together with the corresponding modulation efficiency for each group index value. The insertion loss penalty of the slow wave modulator compared to the conventional modulator can be defined as:

$$IL_{Penalty} = C_p + \left(\alpha_{sw} - \alpha \cdot EF\right) \cdot L_{sw} \tag{3}$$

where C_p are the total coupling losses at the input and output of the slow wave waveguide, α_{sw} and α are the respective propagation losses in the slow wave and conventional rib waveguides, EF is the enhancement factor and L_{sw} is the modulation length. In Fig. 2(f), L_{sw}=1mm, α=4.5dB/mm and the term $C_p + \alpha_{sw} \cdot L_{sw}$ is basically equal to the results shown in Fig. 2(e). It can be seen that the insertion loss penalty linearly increases up to 13 dB for a group index of ~16 but then appears to slightly begin to drop for higher group indices. This is because the enhancement factor improvement dominates over the loss increase and suggests that the insertion loss penalty could be reduced by using very high group indices if this trend were preserved. However, it has been reported [34] that the losses drastically increase for group indices above ~30. This would reverse the suggested trend and yield to a local minimum of insertion loss penalty associated with a maximum enhancement factor. On the other hand, very high group indices would also lead to a strong dependence of the phase shift upon applied voltage as the group index variation with voltage could no longer be considered constant at a given wavelength. Therefore, a comprehensive study should be carried out by analyzing in depth these issues in order to demonstrate whether the use of very high group indices could eventually lead to an enhanced modulation performance together with acceptable insertion losses.

5. High speed performance

In any case, the modulator length may be reduced to minimize the impact of the insertion losses, which in turn would also improve the modulator frequency bandwidth at the expense of a lower modulation depth. The smaller length would also reduce the insertion loss penalty shown in Fig. 2(f), although it is worth noting that this reduction could be limited if the coupling losses dominated over the propagation losses. To provide experimental evidence of the influence of the modulation length over the bandwidth and modulation depth, two 1mm and 0.5mm long slow wave MZI modulators, with respective footprints of 650 (1000x0.650μm^2) and 325μm^2 (1000x0.325μm^2) have been characterized. Transverse electric (TE) polarized light emitted by an external cavity laser (ECL) is injected into the modulator via grating couplers. The transmitted power is optimized through the use of a polarization controller (PC). The small electrical signal delivered by the port 1 of the RF vectorial network analyzer (VNA Agilent E5071C) is coupled a DC bias via a bias-Tee and applied through high speed GSG probes to the travelling wave electrodes terminated externally by a 50 Ω load coupled to a DC block. In addition, a 6V DC bias was applied to drive the slow wave MZI modulator approximately at the quadrature point. The output modulated signal is amplified

#149714 - $15.00 USD Received 22 Jun 2011; revised 22 Jul 2011; accepted 25 Jul 2011; published 5 Oct 2011

with an erbium-doped fiber amplifier (EDFA) and photodetected by a high speed photodiode (XPDV2040R 50 GHz) connected to the port 2 of the RF VNA in order to extract the electro-optical S21 transfer function.

Figure 3(a) shows the normalized electro-optical frequency response of the two MZI slow wave modulators both driven at a group index value of ~11. It can be seen that the 3dB roll-off frequency is improved from ~11 GHz to ~16GHz due to the length reduction of the slow wave phase shifter. In fact, the bandwidth is mainly limited as a result of the velocity mismatch between the electrical and optical signals as the travelling wave (TW) electrode parameters are not properly optimized for the slow light regime. Indeed, as shown in Fig. 3(b), a bandwidth higher than 20GHz was measured in the fast light region for the 1mm long phase shifter, but declines as the group index increases thus imposing a trade-off between bandwidth and modulation efficiency. Additionally, the reduction of the modulation length provides a higher bandwidth owing to the lower influence of the velocity mismatch.

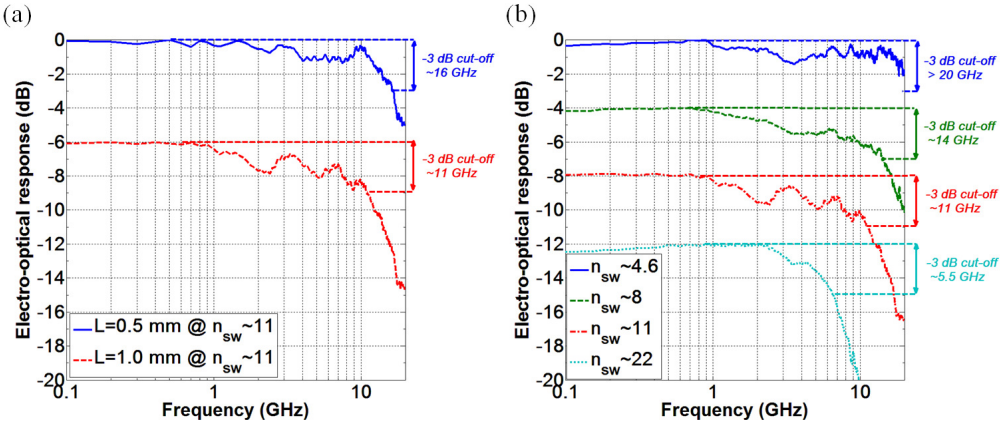

Fig. 3. Slow wave modulator electro-optical response. (a) Normalized electro-optical frequency response of two MZI modulators with respective slow wave phase shifter lengths of 1mm and 0.5mm. Spectra are shifted vertically by 6 dB for clarity. (c) Normalized electro-optical frequency response of the 1mm long slow wave modulator for varying group index. Spectra are shifted vertically by 4 dB for clarity. The 3dB roll-off bandwidth of the TW slow wave modulator is mainly limited as a result of the velocity mismatch between the electrical and optical signals, which imposes a trade-off between bandwidth and modulation efficiency

Electro-optical bandwidth improvement indicates that the maximum data rate our slow wave modulator could handle without degrading the bit error rate (BER) performance is increased accordingly. Data transmission measurements were carried out driving the slow wave modulator with a non-return to zero (NRZ) pseudo-random bit sequence (PRBS) of length 2^{31}-1 delivered by a bit pattern generator (SHF BPG 44E) connected to an external clock. The electrical signal was amplified through a 40 GHz driving amplifier to achieve a voltage swing of ~5 V_{pp} and combined to a 6V DC bias voltage using a bias-tee. In line with our previous electro-optical measurements, the modulating signal was applied to the TW electrodes terminated externally by a 50 Ω resistance coupled to a DC block. The output modulated optical signal was then photodetected by a 40 GHz Digital Communication Analyzer (Infiniium DCA-J 86100C). The BER was measured using an Error Analyzer (SHF EA 44) and evaluated as a function of the optical power received at the photodetector.

The 1mm and 0.5mm long slow wave modulator eye diagrams at 10 Gb/s, 20 Gb/s 30 Gb/s, and 40 Gb/s are depicted respectively in Fig. 4(a), (b), (c) and Fig. 4(d), (e), (f) and (g). In all cases, the eye patterns were measured under identical experimental conditions. In agreement with the measured 1mm long modulator roll-off frequency, the photodetected optical signal is distorted beyond 10Gb/s. Due to the longer rise and fall times, the eye pattern closes up leading to an increasing intersymbol interference (ISI). In addition, the ER is also affected and rapidly decreases from 9.5dB at 10Gb/s to 6.7dB and 4.9dB at 20Gb/s and

#149714 - $15.00 USD Received 22 Jun 2011; revised 22 Jul 2011; accepted 25 Jul 2011; published 5 Oct 2011

30Gb/s, respectively. On the other hand, for the 0.5 mm long slow wave modulator, the eye patterns remain relatively well open at both 10Gb/s and 20Gb/s and noticeable ISI was observed above these data rates. As expected, the ER is reduced compared to the 1mm long slow wave modulator due to the lower achieved phase shift but is in turn less degraded by ISI as the bit rate increases. The measured ERs are 7.6dB, 6.3dB and 5.3dB at 10 Gb/s, 20Gb/s and 30Gb/s respectively. Increasing the speed further up to 40 Gb/s shows that the modulator keeps responding to the electrical driving signal in spite of a noticeable degradation of the eye diagram. The estimated ER at this rate is ~3 dB.

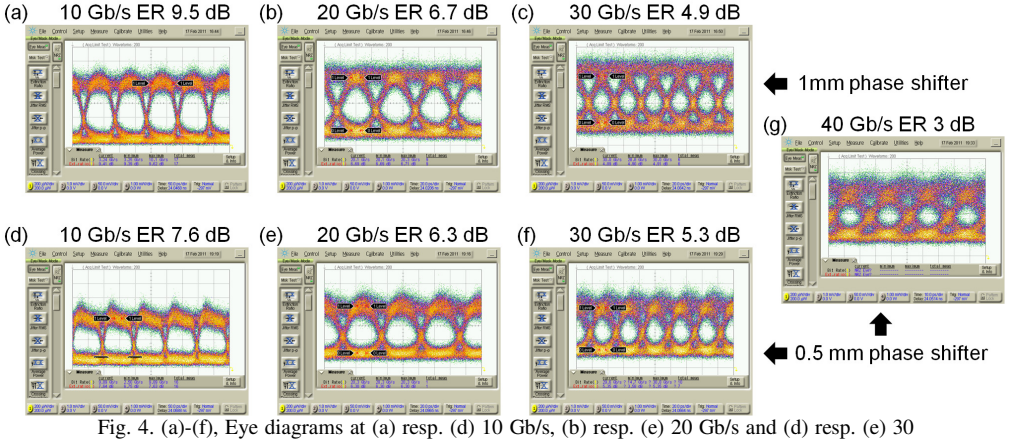

Fig. 4. (a)-(f), Eye diagrams at (a) resp. (d) 10 Gb/s, (b) resp. (e) 20 Gb/s and (d) resp. (e) 30 Gb/s resp. (f) and (g) 40 Gb/s of the 1mm resp. 0.5mm long slow wave modulators.

The BER was also measured to characterize thoroughly the data transmission capability of our slow wave devices. Figure 5 shows the BER results with interpolated linear curves at 10Gb/s and both 10 Gb/s and 20 Gb/s for the 1mm and 0.5mm long modulators, respectively. As expected, we were not able to measure error free operation (BER<10^{-9}) at higher bit rates, as a noticeable error floor caused by ISI arose around BER~10^{-5}, which confirms the data rate limitation imposed by the modulator bandwidth. Furthermore, as a result of the lower ER, the shorter modulator exhibits a power penalty of 2.4dB at 10 Gb/s relative to the longer one, i.e. the overall transmitted optical power must be increased accordingly in order to maintain error free performance, that is the signal integrity. An additional power penalty of 3dB is also required as the data rate increases from 10Gb/s to 20Gb/s in the 0.5mm long slow wave modulator.

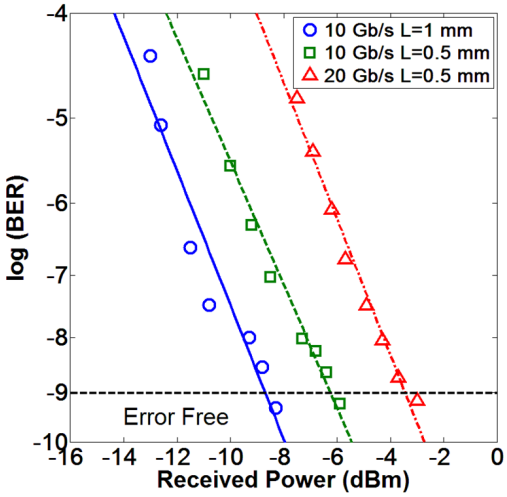

Fig. 5. Bit-error rate (BER) curves at 10Gb/s and respectively 10 Gb/s and 20 Gb/s for the 1mm and 0.5mm long slow wave modulators.

#149714 - $15.00 USD Received 22 Jun 2011; revised 22 Jul 2011; accepted 25 Jul 2011; published 5 Oct 2011

6. Conclusion

Our experimental results have shown the potential for slow light propagation as a means to enhance the modulation efficiency of silicon electro-optical modulators. The main limitation arises from the insertion loss, which may in turn be minimized as a result of the much shorter achievable phase shifter lengths, even for moderate group indices. As a result of the enhanced modulation efficiency, error free modulation up to 20 Gb/s has been demonstrated in a 500μm long CMOS compatible slow wave modulator at a group index of only ~11. Furthermore, the modulator bandwidth could be significantly increased via optimization of the TW electrodes for the slow light regime to ultimately improve the modulation speed to the levels that the *pn* junction is intrinsically capable of achieving. Moreover, the perspective of using higher group indices as well as engineered slow light structures to achieve a constant group index with low losses in a broader wavelength range [36–39] also leaves room for further improvements. Overall, these result confirm the potential groundbreaking impact of slow light in the field of ultra fast and compact silicon modulators.

Acknowledgements

Funding by the European Commission under project HELIOS (photonics electronics functional integration on CMOS), FP7-224312, is acknowledged. P.S. and J.M. also acknowledge financial support from TEC2008-06360 DEMOTEC, TEC2008-06333 SINADEC and PROMETEO-2010-087 R&D Excellency Program (NANOMET). F.Y.G, D.J.T. and G.T.R. are supported by funding received from the UK EPSRC funding body under the grant “UK Silicon Photonics”.

#149714 - $15.00 USD Received 22 Jun 2011; revised 22 Jul 2011; accepted 25 Jul 2011; published 5 Oct 2011